An electrochemical DNA biosensor based on nitrogen-doped graphene/Au nanoparticles for human multidrug resistance gene detection

Mei Chen, Changjun Hou, Danqun Huo, Jing Bao, Huanbao Fa, Caihong Shen

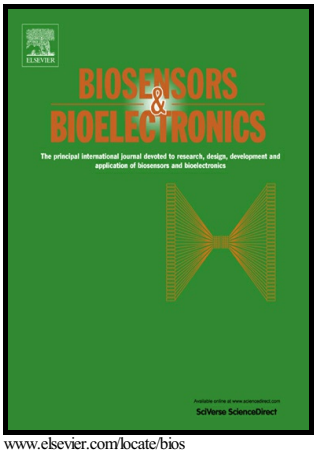

www.elsevier.com/locate/bios

PII: S0956-5663(16)30481-X
DOI: http://dx.doi.org/10.1016/j.bios.2016.05.051
Reference: BIOS8741

To appear in: *Biosensors and Bioelectronic*

Received date: 19 December 2015
Revised date: 19 April 2016
Accepted date: 16 May 2016

Cite this article as: Mei Chen, Changjun Hou, Danqun Huo, Jing Bao, Huanba Fa and Caihong Shen, An electrochemical DNA biosensor based on nitrogen doped graphene/Au nanoparticles for human multidrug resistance gene detectior *Biosensors and Bioelectronic,* http://dx.doi.org/10.1016/j.bios.2016.05.051

An electrochemical DNA biosensor based on nitrogen-doped graphene/Au nanoparticles for human multidrug resistance gene detection

Mei Chen[a], Changjun Hou[a,b]*, Danqun Huo[a], Jing Bao[a], Huanbao Fa[c], Caihong Shen[d]

[a] Key Laboratory of Biorheology Science and Technology, Ministry of Education, College of Bioengineering, Chongqing University, Chongqing 400044, PR China

[b] National Key Laboratory of Fundamental Science of Micro/Nano-Device and System Technology, Chongqing University, Chongqing, 400044, China

[c] College of Chemistry and Chemical Engineering, Chongqing University, Chongqing 400044, China

[d] National Engineering Research Center of Solid-State Brewing, Luzhou, Sichuan, 646000, PR China;

* Corresponding author: Changjun Hou. Tel: +862365112673; fax: +862365102507.

E-mail address: houcj@cqu.edu.cn

Abstract

Multidrug resistance (MDR) has become a major obstacle to the adequate treatment of cancer patients; thus, there is an urgent need for exploring new strategies for early diagnosis of MDR in clinic. Here, we report a novel electrochemical biosensor based on nitrogen-doped graphene nanosheets functionalized with Au nanoparticles (N-G/Au) for sensitive and selective DNA detection. The highly conductive nanocomposite layer was characterized by using scanning and transmission electron microscopy, X-ray photoelectron spectroscopy, and cyclic voltammetry. DNA with thiol groups at the 5′ end was immobilized on the N-G/Au surface via the strong Au–S bond. Differential pulse voltammetry was applied to monitor the target DNA hybridization event using methylene blue as an electrochemical indicator. Under optimal conditions, the biosensor could detect target DNA down to 3.12×10^{-15} M with a linear range from 1.0×10^{-14} to 1.0×10^{-7} M, showing high sensitivity. Further, the sensing strategy was successfully used for detecting *MDR1* DNA in real clinical samples. These results will aid in developing a new portable detection system for

MDR that will allow effective diagnosis in the early stages of related cancer.

Key words: Electrochemical biosensor; DNA detection; Multidrug resistance gene; Nitrogen-doped graphene; Au nanoparticles

1. Introduction

Cancer poses a serious threat to human health worldwide. Although chemotherapy currently generally is an effective treatment option for cancers, the resistance of tumor cells to chemotherapeutic drugs remains a major obstacle for effective cancer treatment (Bebawy et al. 2009). In human cells, expression of multidrug resistance gene 1 (*MDR1*), which encodes a transmembrane efflux pump (P-glycoprotein), leads to decreased intracellular accumulation of lipophilic drugs and increased resistance to such drugs, thus resulting in multidrug resistance (MDR) (Fouladi et al. 2015; Jean et al. 2014). The levels of MDR in cell lines selected *in vitro* have been shown to correlate with the steady-state levels of *MDR1* mRNA and P-glycoprotein (Prateek et al. 2014). Therefore, sensitive detection of MDR may have many potential applications in reliable, early detection for cancer.

Conventional methods to identify MDR include northern and western blotting, flow cytometry, polymerase chain reaction (PCR), and functional MDR assays (Oh et al. 2012; Olesen et al. 2003). Unfortunately, although these approaches are powerful and error-proof, most of them involve unavoidable shortcomings, including time-consuming procedures, high cost and requirement for dedicated instrumentation (Gao et al. 2011). Thus, a simple, specific, and sensitive method for efficient detection and identification of MDR in the clinic is urgently needed. As an alternative to conventional techniques, electrochemical DNA biosensors have attracted considerable interest owing to their intrinsic advantages, including good portability, fast response, and remarkably high sensitivity (Sun et al. 2010). More importantly, a number of DNA biosensors have been developed and extensively applied for the determination of biomarkers (Huang et al. 2014).

To improve the sensitivity and selectivity of biosensors, several methods using signal amplification or different detection technologies have been developed (Luo et al. 2013). In particular, nanomaterial-based systems have been shown to have outstanding efficiency for DNA analysis owing to their ultrahigh surface-to-volume ratio, superior conductivity, and good biological compatibility. Graphene, a single-atom-thick sheet of hexagonally arrayed sp^2-bonded carbon atoms, has been shown to have multiple promising applications in biochemical sensors (Castro Neto et al. 2009; Song et al. 2010). Nitrogen-doped graphene (N-G) is more commonly used than pristine graphene in super capacitors, fuel cells, and field-effect transistors (Ishikawa et al. 2011; Yu et al. 2010) because of its much larger functional surface area, higher ratio of surface-active groups to volume, increased biocompatible C/N microenvironment, higher electrical conductivity, and higher number of chemically active sites for further functionalization with metal nanoparticles (NPs) (Moon et al. 2014; Wei et al. 2009). N-G sheets also serve as good platforms for the loading of nanomaterials (Chen et al. 2012; Zou et al. 2013). Consequently, exploration of the potential of N-G-based composites for biological applications is necessary.

Au NPs are extensively used to amplify hybridization events in DNA hybridization sensing because of their high chemical stability, good biocompatibility, and ability to facilitate electron transfer between biomolecules and electrodes (Liu et al. 2013; Wang et al. 2014). Moreover, Au NPs can form links with several

compounds through Au-NH or Au-S chemical bonds or electrostatic interactions through negative charges (Lu et al. 2012; Zhang and Huang 2012). Numerous attempts have been made to synthesize hybrid structures of graphene with Au NPs for utilization in the field of electrochemical biosensors (Coros et al. 2013; Huang et al. 2015).

Doping graphene with nitrogen atoms can introduce defective sites on the graphene surface to improve electrocatalytic properties. However, to the best of our knowledge, few studies have investigated the electrochemical determination of DNA or nucleic acid hybridization using N-G/Au nanocomposites. Therefore, in this study, we aimed to construct an enzyme-free and label-free electrochemical biosensor using a hybrid nanomaterial composed of an N-G- and Au NPs-modified glassy carbon electrode (GCE) for ultrasensitive detection of DNA. The use of N-G was expected to greatly increase the electrode surface area and electrical conductivity, and the Au NPs were predicted to further enhance the immobilization of the probe DNA and hybridization ability.

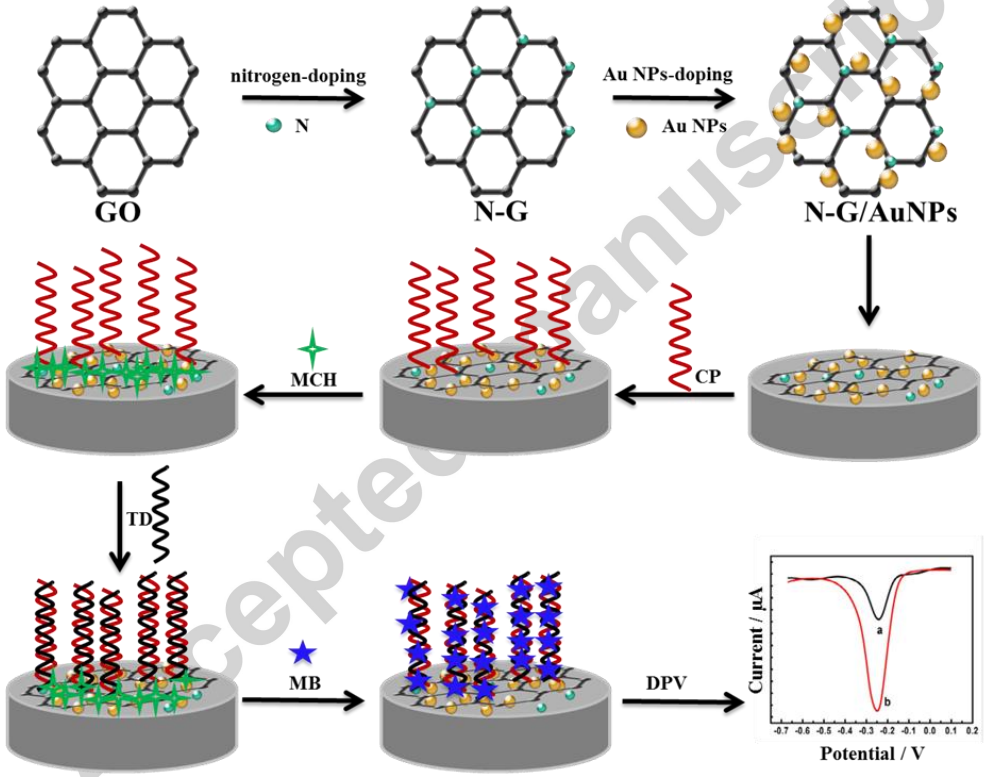

oligonucleotides	Sequences (from 5' to 3')
capture probe (CP)	SH-GCTATAATGCGACAGGAGATAGGCT
complementary target (TD)	CGATATTACGCTGTCCTCTATCCGA
single-base mismatch target (1MT)	CGATATTACGCAGTCCTCTATCCGA
three-base mismatch target (3MT)	CCATATAACGCAGTCCTCTATCCGT
non-complementary sequence (NC).	TTGTCCAGGTAGGAGCACAGGATG
PCR Primer 1	CAGGAGATAGGCTGGTTTGATGT
PCR Primer 2	TTAGCTTCCAACCACGTGTAAATC

Figure 1. Schematic representation of the electrochemical DNA biosensor. The sequences of the oligonucleotides used in this study are listed below the figure.

2. Experimental

2.1. Apparatus and materials

Electrochemical measurements were performed on a CHI 600D electrochemical workstation. Samples were morphologically characterized using an FEI Nova 400 field emission scanning electron microscope (FESEM) and a ZEISS LIBRA 200 transmission electron microscope (TEM). A Bruker D8 Advance X-ray diffractometer was used for XRD. XPS measurements were conducted using a 5300 ESCA instrument. PCR was carried out using an Eppendorf Mastercycler Gradient PCR system, and gel images were recorded on a Bio-Rad imaging system. The quantitative real-time PCR (qRT-PCR) analysis was performed using a Realplex (Eppendorf, Germany). Leukemic cell samples from three patients were collected from the cell resource center of the Chinese Academy of Sciences (Shanghai, China). All of the oligonucleotides and primers (Fig. 1) were synthesized and purified by Sangon Biological Engineering Tech. Co. Ltd and were diluted with Tris-ethylenediaminetetraacetic acid (TE) buffer (pH 7.4). Methylene blue (MB), 6-mercapto-1-hexanol (MCH), Tris-HCl, and Na_2EDTA were purchased from Sigma-Aldrich (St. Louis, MO, USA). All other chemicals were of analytical grade. Deionized (DI) water was produced using a Millipore system.

2.2. Preparation of N-G and N-G/AuNPs nanocomposites

Graphite was first oxidized to graphene oxide (GO) using a modified Hummers' method as described previously (Liu et al. 2010). The N-G was synthesized according to a previous study (Long et al. 2010). Typically, 30 mL of a 2.0 mg mL^{-1} GO solution was used, the pH was adjusted to 10 with 30% ammonia, and 2 mL of hydrazine hydrate was added. After stirring for 10 min, the solution was heated at 200°C for 3 h.

Au NP-decorated N-G (N-G/Au) was synthesized by the reduction of $HAuCl_4$ on the N-G surface using ethylene glycol (EG) as the reducing agent. In a typical synthesis protocol, 0.02 g N-G was suspended in 21 mL DMF with the aid of ultrasonication for 30 min. Then, a mixture of 14 mL of 0.01 M $HAuCl_4$ and 40 mL of EG was added to the suspension. After magnetically stirring for 30 min, the solution was heated at 80°C under constant stirring. After a 10-h reaction, the product was washed several times with ethanol/water, and dried at 70°C.

2.3. Fabrication of the DNA electrochemical biosensor

The GCE was wet-polished down to a mirror-like surface. Then, 5 μL of a 2 mg mL^{-1} N-G/Au suspension, which was prepared as described above, was coated on the electrode surface to obtain the N-G/Au/GCE complex, and dried in air at room temperature. The GO (2 mg mL^{-1})-modified GCE (GO/GCE) and the N-G (2 mg mL^{-1})-modified GCE (N-G/GCE) were prepared in the same way.

For immobilization of 5'-thiolated ssDNA used as the capture probe (CP), 5 μL of ssDNA (1×10^{-6} M) solution was drop-cast to cover the modified electrode and incubated for 2 h at 25 °C. The CP was immobilized on the N-G/Au/GCE through the strong Au–S bond (Zhang et al. 2014) and the electrostatic interaction with the positively charged Au NPs (Lu et al. 2013). Subsequently, the CP-modified electrode (CP/N-G/Au/GCE) was treated with 1.0 mM MCH for 1 h to eliminate nonspecifically adsorbed ssDNA molecules. MCH used as a blocking agent to fix CP/N-G/Au on the glassy carbon surface and to maintain proper orientation of the ssDNA for sufficient recognition ability (Cheng et al. 2012).

2.4. Hybridization and electrochemical measurements

Hybridization was performed by immersing the CP/N-G/Au/GCE into 0.01 M PBS containing various concentrations of target DNA (TD) at 30°C for 1 h. The hybridized electrode (CP-TD/N-G/Au/GCE) was rinsed with PBS to remove any non-specifically adsorbed DNA and was used for electrochemical measurements. The procedures for biosensor fabrication and DNA detection are schematically shown in Fig. 1. The CP-TD/Au/N-G/GCE was incubated in a 20-μM MB solution (containing 20 mM NaCl) for 20 min, and then washed with 0.1 wt% sodium dodecyl sulfate in PBS (pH 7.0). The electrochemical response was measured by differential pulse voltammetry (DPV).

2.5. Preparation of real DNA samples and PCR

Total RNA was extracted from cryopreserved leukemic cell samples using a guanidinium thiocyanate-phenol chloroform method with TRIzol reagent according to the manufacturer's recommendations. First-strand cDNA was synthesized using SuperScript III reverse transcriptase. The thermal cycling conditions were as follows: 94°C for 2 min; 40 cycles of 94°C for 30 s, 60°C for 30 s, and 72°C for 1 min; and a final extension at 72°C for 10 min. Amplicons were visualized under ultraviolet light after running 6 μL of the reaction mixture on an agarose gel (2%) containing 1 mg mL^{-1} ethidium bromide (EtBr). The qRT-PCR analysis was performed in a total reaction volume of 20 μL containing 2 μL of the diluted reaction mixture and 18 μL Bio-Rad iQ SYBR Green Supermix (Takara, Japan). Data expressed here as relative levels were standardized to a reference gene *B-actin.* All the experiment repeated three times. The PCR products were immersed in 0.2 M NaOH and 5 mM EDTA (37℃)for 30 minutes and the precipitate denatured DNA in ethanol to obtain denatured ssDNA.

3. Results and discussion

3.1. Characterization of the N-G and N-G/AuNPs nanocomposites

Addition of metallic nanoparticles to N-G could provide a feasible pathway for electron transfer and enhance the intrinsic electrocatalytic activity of N-G through electronic structure modification (Zhou et al. 2010), which is favorable for the fabrication of electrochemical DNA biosensors.

As shown in Fig. 2, the N-G consisted of overlapping transparent layers and silk-like parts, in addition to wrinkles and folds (Fig. 2A), indicating that the high surface/volume ratio and the two-dimensional structure of the graphene were well maintained. After the reduction of $HAuCl_4$ by EG, numerous aggregated Au NPs were distributed over the surface of the N-G nanosheets (Fig. 2B). The N-G/AuNPs hybrid was decorated with uniform Au NPs, which further increased the conductivity of the electrode. TEM characterization confirmed the morphology of the N-G (Fig. 2C, D) and N-G/AuNPs (Fig. 2E). The high-resolution TEM image showed an interplanar spacing of approximately 0.24 nm, which was in good agreement with the d-spacing of the (111) lattice plane of Au (Fig. 2F).

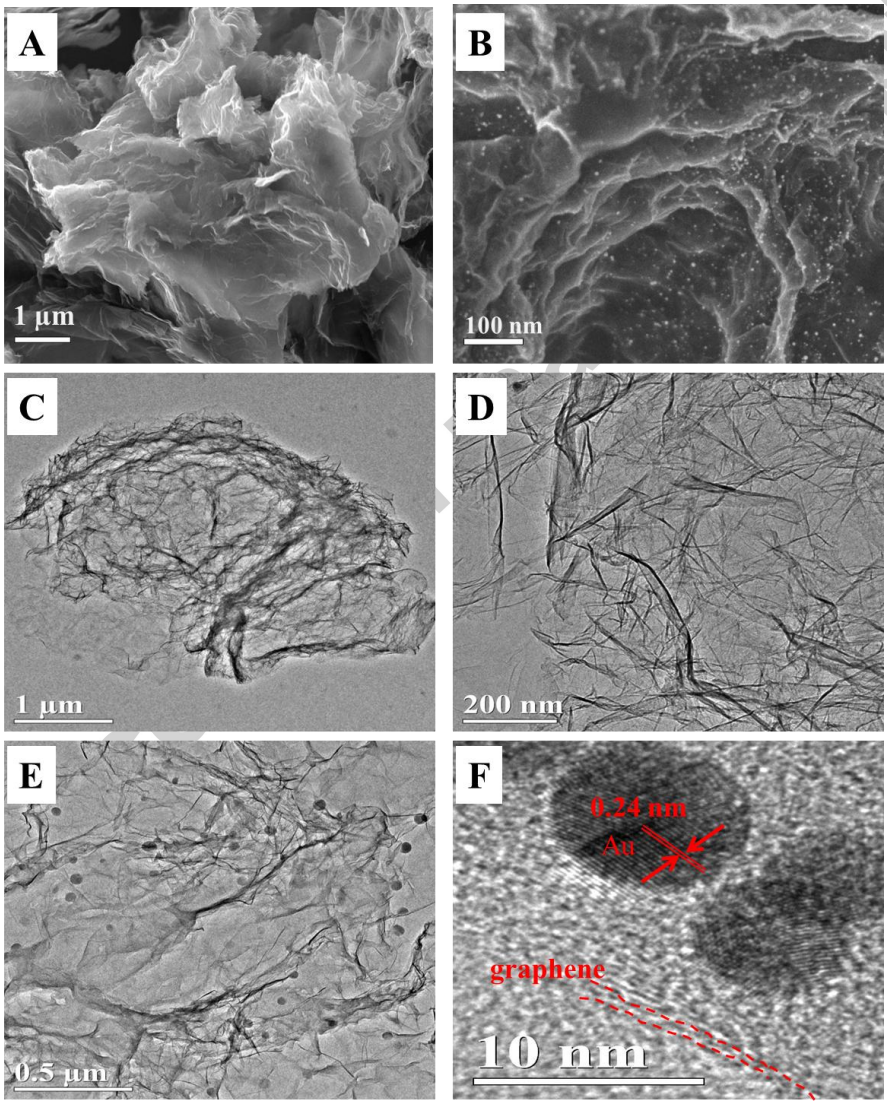

Figure 2. (A, B) SEM images of N-G and N-G/Au. (C, D) TEM images of N-G. (E, F) TEM and high-resolution TEM images of N-G/Au.

XPS analysis was carried out to analyze the surface chemical composition and status of the N-G and N-G/Au further (Fig. 3A). The XPS spectra exhibited distinct C 1s, N 1s, and O 1s peaks for both samples. The N 1s peak appeared at approximately 400 eV, indicating successful doping of N into the graphene. The N/C atomic ratios for N-G and N-G/Au were calculated to be 6% and 4.5%, respectively. The different O/C atomic ratios may have resulted from the nonuniform N-G surface after Au deposition. Fig. 3B illustrates the high-resolution N 1s spectrum of the composition of the N-G/Au. The N 1s spectrum could be clearly deconvoluted into three individual peaks, which were attributed to pyridine N, pyrrolic N, and graphite N (Wang et al. 2010). In addition, Au 4f peaks were observed at binding energies of 84.0 and 87.6 eV (Fig. 3C), which correspond to Au $4f_{7/2}$ and $4f_{5/2}$, respectively (He et al. 2011), confirming the formation of metallic Au on the N-G/Au composite. The XRD patterns of N-G and N-G/Au are shown in Fig. 3D. The peak at 24° for the N-G sample was assigned to the hexagonal graphite structure C (0 0 2). For N-G/Au, additional peaks observed at 38.3°, 44.5°, 64.7°, and 77.6° corresponded to the (1 1 1), (2 0 0), (2 2 0), and (3 1 1) crystal planes, respectively, of the Au NPs.

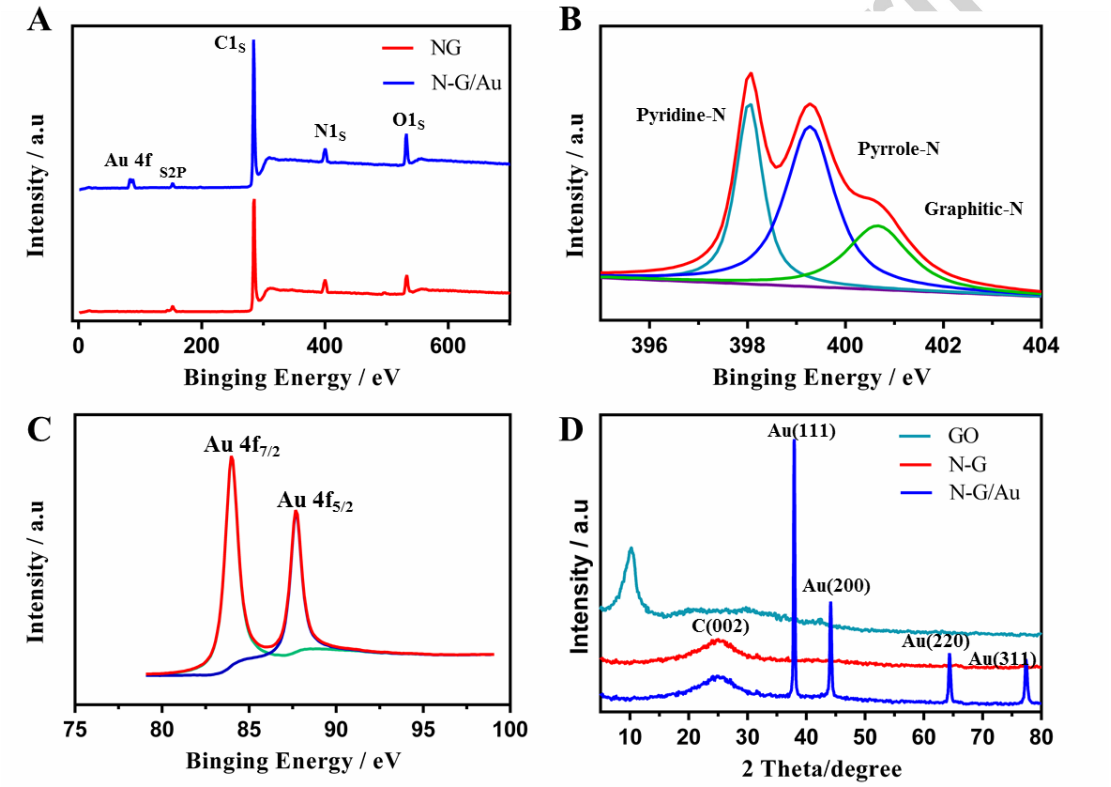

Figure 3. (A) XPS spectra of N-G and N-G/Au. (B) High-resolution N 1s XPS spectrum of N-G/Au. (C) Au 4f XPS spectrum of N-G/Au. (D) XRD patterns of GO, N-G/Au, and N-G.

3.2. Electrochemical characterization of the modified electrodes

Cyclic voltammetry (CV) is an effective and convenient method for probing the features of a modified electrode surface. As shown in Fig. 4, the peak current obtained when GO was assembled on the surface of GCE (green curve) was substantially lower

than that for bare GCE (black curve). When N-G was assembled on the surface of GCE, the peak current clearly increased (red curve), indicating that N-G served as an ideal electrically conductive material accelerating the electron transfer rate of $[Fe(CN)_6]^{3-/4-}$. After attachment of the N-G/Au hybrid material on the GCE surface, the CV peak current clearly increased further (blue curve), demonstrating the good catalytic ability of the composites. These characteristics of the oxidation peak current of N-G/Au/GCE indicate that the unique electrical performance of the N-G/Au composite increased the electrode active area, which is beneficial for improvement of the sensitivity of the biosensor.

The reversibility and peak current of $[Fe(CN)_6]^{3-/4-}$ decreased after immobilization of CP DNA on the NG/Au/GCE composite (light blue curve). This was due to the electrostatic repulsion between the negatively charged HS-ssDNA and $[Fe(CN)_6]^{3-/4-}$. After the CP/N-G/Au/GCE was hybridized with the complementary target DNA (TD), the peak current decreased further (magenta curve), which suggested that introduction of complementary DNA may increase the negative charge, consequently increasing the repellence of redox species. These results confirmed that the biosensor functioned as proposed in the schematic outlined in Fig. 1.

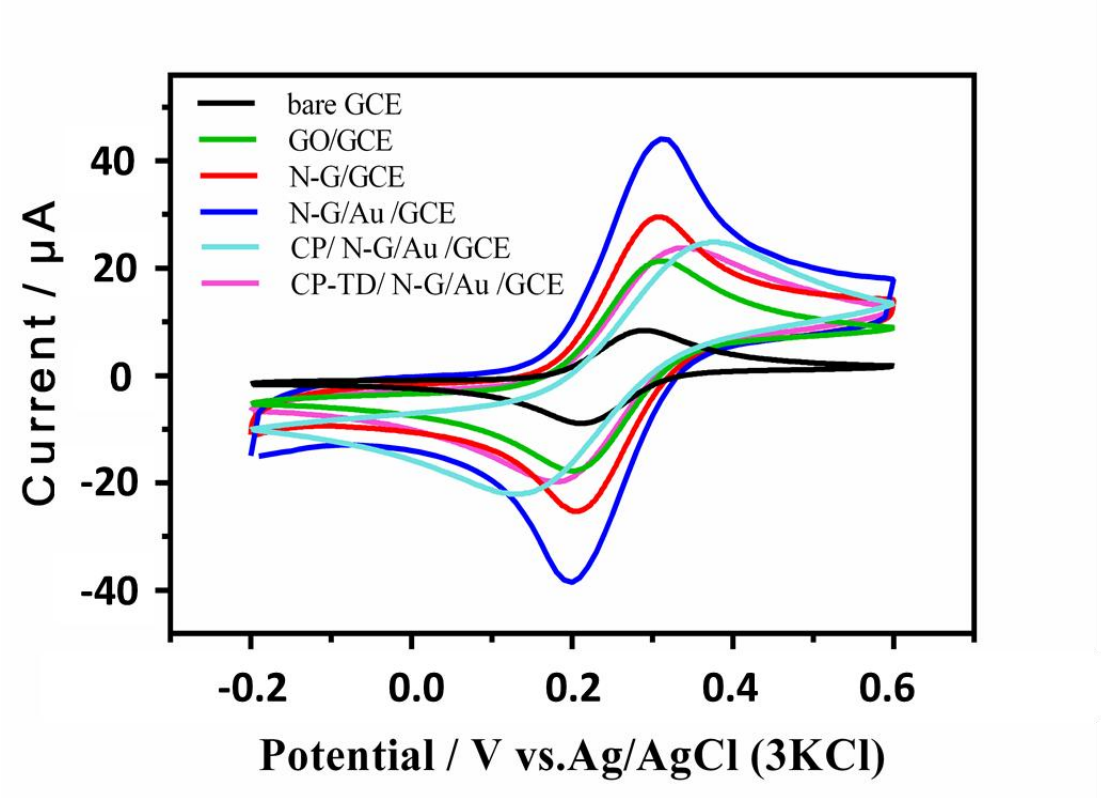

Figure 4. Cyclic voltammograms of differentially modified electrodes in 1.0 mM $Fe(CN)_6^{3-/4-}$ and 0.1 M KCl solution at a scan rate of 100 mV/s. Bare GCE (black); GO/GCE (green); N-G/GCE (red); N-G/Au/GCE (blue); CP/N-G/Au/GCE (light blue); CP-TD/N-G/Au/GCE (magenta).

3.3. Optimization of assay conditions

Experimental conditions were optimized to achieve high analytical performance.

Spectroscopic studies have demonstrated that MB intercalates into the DNA double helix; therefore, MBhas been widely used as an electrochemical indicator in DNA hybridization detection (Lin et al. 2014). As shown in Fig. S1A, the peak current of MB changed with increase in the reaction time in the range of 0–3 h. The response increased significantly from 0 to 2 h, and reached a plateau after 2 h, suggesting that most of the probe ssDNA was immobilized on the electrode by 2 h. Therefore, 2 h was set as the optimal reaction time.

Next, the effects of hybridization time and temperature of the CP DNA and the TD were evaluated (Fig. S1B). When the hybridization temperature was fixed at 30 °C, the peak current of MB obviously increased from 0 to 50 min and remained stable thereafter, indicating that the hybridization reaction was completed within 50 min. The effect of hybridization temperature on the peak current of MB was tested in the range of 20–60°C and the largest peak current was observed at 30°C (Fig. S1C). Thus, we used 50 min and 30 °C in the subsequent experiments.

The concentration and incubation time of the hybridization indicator can also influence the performance of a DNA biosensor. The current response stabilized at an MB concentration $\geq 2.0 \times 10^{-5}$ M (Fig. S1D). Therefore, 2.0×10^{-5} M MB was employed as the indicator. The peak current also increased significantly with increase in incubation time from 0 to 20 min (Fig. S1E). No further increase in current was observed with longer incubation, indicating that saturation was reached within 20 min. Thus, the incubation time with MB was set at 20 min.

3.4. Sensitivity for target detection

The analytical performance of the DNA biosensor was investigated under the optimal conditions. As shown in Fig. 5, the DPV response linearly increased with the logarithm of TD concentration from 1.0×10^{-7} to 1.0×10^{-14} M and the corresponding regression equation was ΔI (μA) = 26.91 + 1.889 × lg c (M) with a correlation coefficient of 0.9935. The detection limit, calculated as three times the standard deviation of the blank sample measurements, was approximately 3.12×10^{-15} M (at an S/N of 3). A comparison of the performance of the present biosensor with that of previously reported sensors is provided in Table S1, which demonstrated that the present method had a broader linear range and a lower detection limit than other methods. Hence, N-G/Au-modified GCE was confirmed to be an efficient electrochemical sensing platform. These characteristics may be attributed to the combination of the high electrochemical activity of N-G and high conductivity of Au NPs.

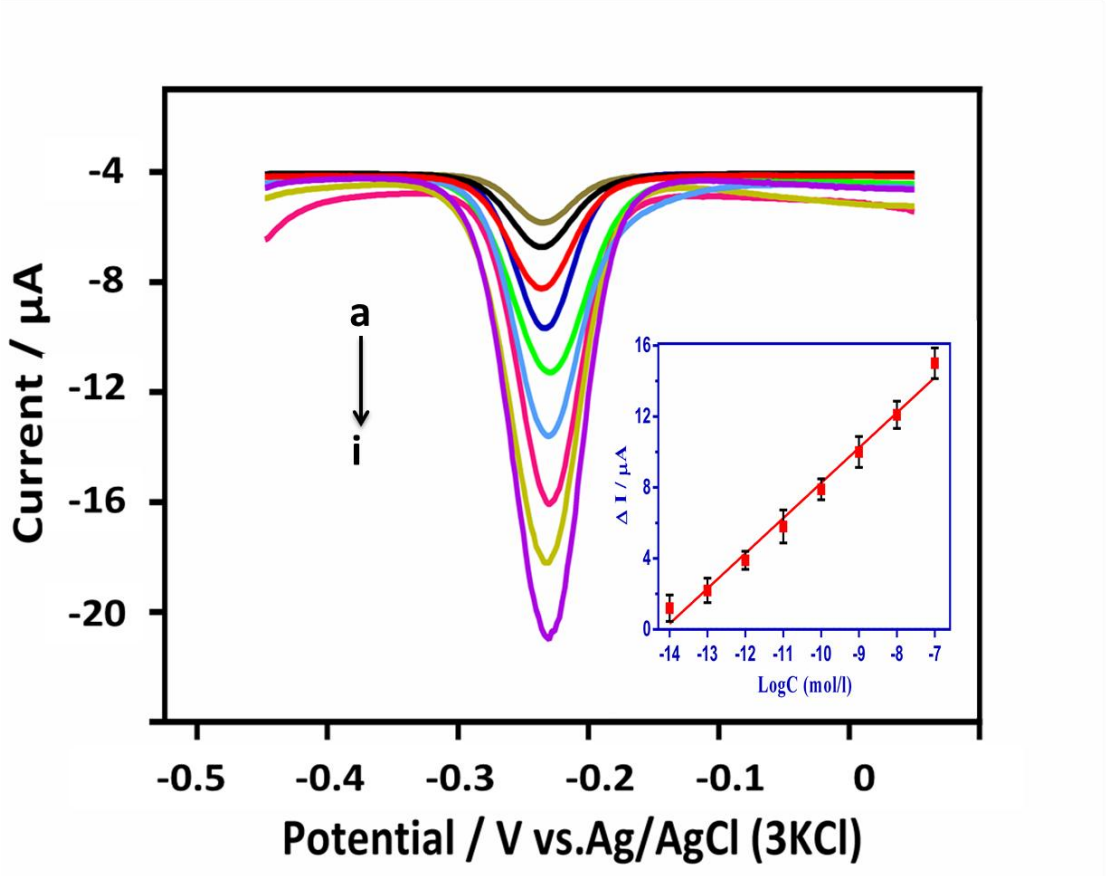

Figure 5. DPV curves after hybridization with different concentrations of TD (0, 1.0×10^{-14}, 1.0×10^{-13}, 1.0×10^{-12}, 1.0×10^{-11}, 1.0×10^{-10}, 1.0×10^{-9}, 1.0×10^{-8}, and 1.0×10^{-7} M, curves a–i, respectively). Inset, plot of peak current versus log of target ssDNA concentration.

3.5. Selectivity, reproducibility, and stability of the DNA sensor

To investigate the selectivity of the biosensor, four types of DNA sequences, that is, TD, single-base mismatch target (1MT), three-base mismatch target (3MT), and noncomplementary sequence (NC), were selected for evaluation. Fig. S2A shows the peak currents for the blank and the four types of DNA sequences. The concentration of TD was 1.0×10^{-12} M, and that of the other DNA sequences was 1.0×10^{-9} M. Although the concentration of disrupted DNA was higher than that of TD, the DPV signal of 1MT was approximately one-third that of TD. The difference between 1MT and 3MT indicated that the base mismatch prevented completion of hybridization. A similar result was obtained for NC, suggesting that the NC DNA could not hybridize with CP and that the response of the mismatched DNA was induced by nonspecific adsorption of ssDNA on the electrode surface. These results demonstrated the good selectivity of the fabricated DNA biosensor.

The reproducibility of the biosensor was also investigated. Five DNA biosensors were prepared for detecting the TD sequence at 1.0×10^{-9} M. The relative standard deviation of the measurements for the five electrodes was 4.1%, which shows the high reproducibility of the DNA detection. Similarly, the stability of the biosensor was

investigated over the course of 1 week (one measurement per day) using five biosensors independently. The values obtained showed no distinct changes (Fig. S2B). The good stability may be attributed to the fact that the DNA sequences were attached firmly onto the surface of the N-G/Au nanocomposite film.

3.6. Evaluation with a clinical sample

To prove that the fabricated biosensor could be used for sensitive detection of actual samples, *MDR1* DNA from - real clinical samples was examined with the sensor. First, total RNA was extracted from three cryopreserved leukemic cell samples. Detection of the RNA by agarose gel electrophoresis is shown in Fig. 6A. After first-strand cDNA synthesis, the *MDR1* gene was amplified by PCR and products were electrophoresed on an agarose gel. The PCR product migrated at the expected size of 1590 bp (Fig. 6B). The data from quantitative real-time PCR analysis showed the relative expression levels of *MDR1* in three samples (Fig. 6C), confirming the identities of the RT-PCR products.

Gel electrophoresis did not allow effective detection of the *MDR1* PCR products at concentrations below 1.0×10^{-11} M due to the low EtBr staining efficiency for ssDNA (Fig. 6D). Next, we applied our electrochemical DNA biosensor to analyze the PCR products of the *MDR1* gene (0–1.0×10^{-14} M). The responses of the biosensor to different dilutions of the PCR sample are shown in Fig. E. The fabricated DNA biosensor could detect *MDR1* DNA at a concentration as low as 1.0×10^{-14} M, which was much below the detection limit of the PCR system. The PCR method has distinct advantages, such as visualization, but is also often associated with false-positive signals, limiting its use in laboratories. The proposed method overcomes several inherent disadvantages of traditional PCR methods owing to the use of a specific DNA probe. Furthermore, the detection procedure of the proposed method could be completed within 3.5 h. Compared with conventional culture methods, which require at least 24–32 h (Nasilowska-Adamska et al. 2014; Sun et al. 2009), our method was more facile and less time-consuming. The proposed strategy exhibited high sensitivity, specificity, and speed, showing its good potential as a practical tool for *MDR1* DNA detection. Moreover, the methodology can be extrapolated to other cancer-related genes with the use of appropriate DNA probes.

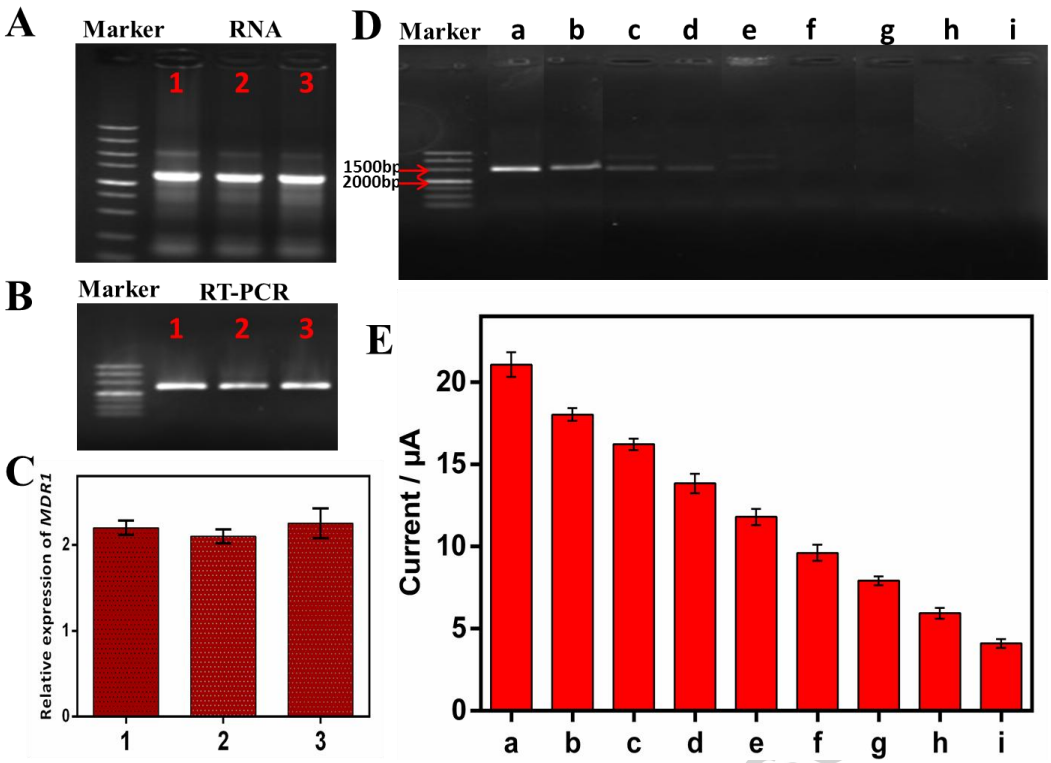

Figure 6. (A) Gel electrophoresis of total RNA. (B) Gel electrophoresis of *MDR1* PCR products. (C) qRT-PCR shown as relative expression levels of *MDR1* normalized by *B-actin*. (D) Gel electrophoresis of *MDR1* PCR products serially diluted from 1.0×10^{-7} to 1.0×10^{-14} M (a–h) and blank (i). (E) DPV peak currents responding to *MDR1* PCR products serially diluted from 1.0×10^{-7} to 1.0×10^{-14} M (a–h) and blank (i). Standard error bars represent three replicates.

4. Conclusions

A sensitive DNA electrochemical sensor based on N-G/Au/GCE for the human *MDR1* gene was successfully fabricated for the first time. The N-G/Au-modified GCE not only accelerated electron transfer but also exhibited high electrochemical activity, significantly enhancing the signal detection. Owing to the large specific area and good conductivity of the N-G/Au, the new DNA biosensor showed a wide linear range and low detection limit for detection of the *MDR1* gene with high selectivity and good stability. Moreover, this method could detect *MDR1* DNA at a concentration as low as 1.0×10^{-14} M in real samples. Together, these data indicated that the designed DNA biosensor—without requirement for enzymes or labels—shows great potential in DNA analysis. It is expected to aid in the development of a new portable system for effective diagnosis of cancer. Future efforts in our laboratory will be directed toward this goal.

Acknowledgements

The authors would like to acknowledge the financial support from National Natural Science Foundation of China (N.O. 81271930, 81171414), Chongqing Graduate

Student Research Innovation Project (N.O. CYB14028), Key Technologies R&D Program of China (N.O. 2014BAD07B02) and Brew Microorganisms Technology and Application of Key Laboratory Project in Sichuan Province (N.O. NJ2014-03).

References

Bebawy, M., Combes, V., Lee, E., Jaiswal, R., Gong, J., Bonhoure, A., Grau, G.E.R., 2009. Membrane microparticles mediate transfer of P-glycoprotein to drug sensitive cancer cells. Leukemia 23(9), 1643-1649.

Castro Neto, A.H., Guinea, F., Peres, N.M.R., Novoselov, K.S., Geim, A.K., 2009. The electronic properties of graphene. Rev Mod Phys 81(1), 109-162.

Chen, P., Xiao, T.Y., Li, H.H., Yang, J.J., Wang, Z., Yao, H.B., Yu, S.H., 2012. Nitrogen-Doped Graphene/ZnSe Nanocomposites: Hydrothermal Synthesis and Their Enhanced Electrochemical and Photocatalytic Activities. Acs Nano 6(1), 712-719.

Cheng, W., Ding, S.J., Li, Q., Yu, T.X., Yin, Y.B., Ju, H.X., Ren, G.S., 2012. A simple electrochemical aptasensor for ultrasensitive protein detection using cyclic target-induced primer extension. Biosens Bioelectron 36(1), 12-17.

Coros, M., Biris, A.R., Pogacean, F., Tudoran, L.B., Neamtu, C., Watanabe, F., Biris, A.S., Pruneanu, S., 2013. Influence of chemical oxidation upon the electro-catalytic properties of graphene-gold nanoparticle composite. Electrochim Acta 91, 137-143.

Fouladi, R., Schurmann, C., Bessonov, K., Vert, J.P., Loos, R.J.F., Van Steen, K., 2015. A novel gene-based analysis method based on MB-MDR. Genet Epidemiol 39(7), 548-548.

Gao, H., Qi, X., Chen, Y., Sun, W., 2011. Electrochemical deoxyribonucleic acid biosensor based on the self-assembly film with nanogold decorated on ionic liquid modified carbon paste electrode. Ana Chim Acta 704(1-2), 133-138.

He, F.A., Fan, J.T., Song, F., Zhang, L.M., Chan, H.L.W., 2011. Fabrication of hybrids based on graphene and metal nanoparticles by in situ and self-assembled methods. Nanoscale 3(3), 1182-1188.

Huang, H., Bai, W., Dong, C., Guo, R., Liu, Z., 2015. An ultrasensitive electrochemical DNA biosensor based on graphene/Au nanorod/polythionine for human papillomavirus DNA detection. Biosens Bioelectron 68, 442-446.

Huang, K.-J., Liu, Y.-J., Wang, H.-B., Wang, Y.-Y., 2014. A sensitive electrochemical DNA biosensor based on silver nanoparticles-polydopamine@graphene composite. Electrochim Acta 118, 130-137.

Ishikawa, R., Bando, M., Morimoto, Y., Sandhu, A., 2011. Doping graphene films via chemically mediated charge transfer. Nanoscale Res Lett 6(1), 111.

Jean, M., Behhammadi, M., Sidique, A., Jeandupeux, D., Merzouki, A., Buschmann, M.D., 2014. P-Glycoprotein Knock-Down by Chitosan/MDR1-siRNA Nanoparticles Increases Sensitivity to Chemotherapeutics. Mol Ther 22, S259-S259.

Lin, C.S., Wu, Y.F., Luo, F., Chen, D.M., Chen, X., 2014. A label-free electrochemical DNA sensor using methylene blue as redox indicator based on an exonuclease III-aided target recycling strategy. Biosens Bioelectron 59, 365-369.

Liu, F., Choi, J.Y., Seo, T.S., 2010. Graphene oxide arrays for detecting specific DNA hybridization by fluorescence resonance energy transfer. Biosens Bioelectron 25(10), 2361-2365.

Liu, X.Q., Zhang, J.M., Liu, S.H., Zhang, Q.Y., Liu, X.H., Wong, D.K.Y., 2013. Gold Nanoparticle Encapsulated-Tubular TIO2 Nanocluster As a Scaffold for Development of Thiolated Enzyme Biosensors.

Anal Chem 85(9), 4350-4356.

Long, D.H., Li, W., Ling, L.C., Miyawaki, J., Mochida, I., Yoon, S.H., 2010. Preparation of Nitrogen-Doped Graphene Sheets by a Combined Chemical and Hydrothermal Reduction of Graphene Oxide. Langmuir 26(20), 16096-16102.

Lu, J.J., Liu, S.Q., Ge, S.G., Yan, M., Yu, J.H., Hu, X.T., 2012. Ultrasensitive electrochemical immunosensor based on Au nanoparticles dotted carbon nanotube-graphene composite and functionalized mesoporous materials. Biosens Bioelectron 33(1), 29-35.

Lu, X.C., Dong, X., Zhang, K.Y., Han, X.W., Fang, X., Zhang, Y.Z., 2013. A gold nanorods-based fluorescent biosensor for the detection of hepatitis B virus DNA based on fluorescence resonance energy transfer. Analyst 138(2), 642-650.

Luo, C.H., Tang, H., Cheng, W., Yan, L., Zhang, D.C., Ju, H.X., Ding, S.J., 2013. A sensitive electrochemical DNA biosensor for specific detection of Enterobacteriaceae bacteria by Exonuclease III-assisted signal amplification. Biosens Bioelectron 48, 132-137.

Moon, J., An, J., Sim, U., Cho, S.P., Kang, J.H., Chung, C., Seo, J.H., Lee, J., Nam, K.T., Hong, B.H., 2014. One-step synthesis of N-doped graphene quantum sheets from monolayer graphene by nitrogen plasma. Adv Mater 26(21), 3501-3505.

Nasilowska-Adamska, B., Solarska, I., Paluszewska, M., Malinowska, I., Jedrzejczak, W.W., Warzocha, K., 2014. FLT3-ITD and MLL-PTD influence the expression of MDR-1, MRP-1, and BCRP mRNA but not LRP mRNA assessed with RQ-PCR method in adult acute myeloid leukemia. Ann Hematol 93(4), 577-593.

Oh, S., Lee, J., Kwon, M.S., Weir, B., Ha, K., Park, T., 2012. A novel method to identify high order gene-gene interactions in genome-wide association studies: Gene-based MDR. Bmc Bioinformatics 13.

Olesen, L.H., Norgaard, J.M., Pallisgaard, N., Bukh, A., Hokland, P., 2003. Validation and clinical implication of a quantitative real-time PCR determination of MDR1 gene expression: comparison with semi-quantitative PCR in 101 patients with acute myeloid leukemia. Eur J Haematol 70(5), 296-303.

Prateek, B., Masih, S., Rani, S., Varma, N., Binota, J., Bansal, D., Marwaha, R.K., 2014. Gene Expression of Multi Drug Resistance Protein (Mdr-1), Multi Drug Related Protein (Mrp) and Lung Resistance Protein (Lrp) in Pediatric Acute Lymphoblastic Leukemia Cases. Pediatr Blood Cancer 61, S264-S264.

Song, Y.J., Qu, K.G., Zhao, C., Ren, J.S., Qu, X.G., 2010. Graphene Oxide: Intrinsic Peroxidase Catalytic Activity and Its Application to Glucose Detection. Adv Mater 22(19), 2206-+.

Sun, H., Choy, T.S., Zhu, D.R., Yam, W.C., Fung, Y.S., 2009. Nano-silver-modified PQC/DNA biosensor for detecting E. coli in environmental water. Biosens Bioelectron 24(5), 1405-1410.

Sun, W., Qin, P., Gao, H., Li, G., Jiao, K., 2010. Electrochemical DNA biosensor based on chitosan/nano-V 2 O 5/MWCNTs composite film modified carbon ionic liquid electrode and its application to the LAMP product of Yersinia enterocolitica gene sequence. Biosens Bioelectron 25(6), 1264-1270.

Wang, Y., Shao, Y.Y., Matson, D.W., Li, J.H., Lin, Y.H., 2010. Nitrogen-Doped Graphene and Its Application in Electrochemical Biosensing. Acs Nano 4(4), 1790-1798.

Wang, Y.L., Li, X.J., Cao, W., Li, Y.Y., Li, H., Du, B., Wei, Q., 2014. Ultrasensitive sandwich-type electrochemical immunosensor based on a novel signal amplification strategy using highly loaded toluidine blue/gold nanoparticles decorated KIT-6/carboxymethyl chitosan/ionic liquids as signal labels. Biosens Bioelectron 61, 618-624.

Wei, D., Liu, Y., Wang, Y., Zhang, H., Huang, L., Yu, G., 2009. Synthesis of N-doped graphene by chemical vapor deposition and its electrical properties. Nano Lett 9(5), 1752-1758.

Yu, S.S., Zheng, W.T., Wang, C., Jiang, Q., 2010. Nitrogen/Boron Doping Position Dependence of the

Electronic Properties of a Triangular Graphene. Acs Nano 4(12), 7619-7629.

Zhang, P., Wu, X., Chai, Y., Yuan, R., 2014. An electrochemiluminescent microRNA biosensor based on hybridization chain reaction coupled with hemin as the signal enhancer. Analyst 139(11), 2748-2753.

Zhang, Y.Z., Huang, L., 2012. Label-free electrochemical DNA biosensor based on a glassy carbon electrode modified with gold nanoparticles, polythionine, and graphene. Microchim Acta 176(3-4), 463-470.

Zhou, Y.K., Neyerlin, K., Olson, T.S., Pylypenko, S., Bult, J., Dinh, H.N., Gennett, T., Shao, Z.P., O'Hayre, R., 2010. Enhancement of Pt and Pt-alloy fuel cell catalyst activity and durability via nitrogen-modified carbon supports. Energ Environ Sci 3(10), 1437-1446.

Zou, F., Hu, X., Sun, Y., Luo, W., Xia, F., Qie, L., Jiang, Y., Huang, Y., 2013. Microwave-Induced in situ synthesis of Zn2GeO4/N-doped graphene nanocomposites and their lithium-storage properties. Chemistry 19(19), 6027-6033.

Highlights

1 This work constructs an ultrasensitive electrochemical DNA biosensor.

2 Nitrogen-doped graphene (NG) and Au NPs composites providing a promising platform for DNA probe immobilization.

3 DNA was detected sensitively due to the large specific area of the NG/ Au NPs which provide high capturing for molecular recognition elements.

4 This biosensor has been used for detection of *MDR* DNA in clinical samples.